Facile tuning of plasmon bands in hollow silver nanoshells using mild reductant and mild stabilizer

Satarupa Pattanayak[a], *Amiya Priyam*[a,*] *and Pradip Paik*[b,c]

Supplementary Information

Optimization of synthesis temperature

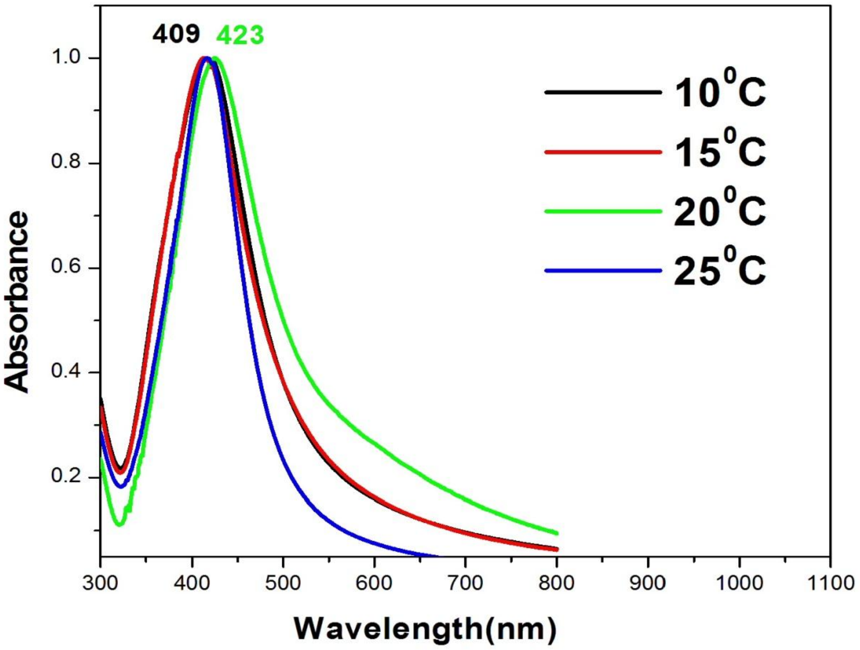

Figure S1. The effect of synthesis temperature on the UV-Vis spectra of silver nanoparticles prepared by reduction of Ag_2O NPs at basic pH. (Stabilizer : citrate; Reducing agent :hydrazine hydrate)

The reduction of Ag_2O NPs was carried out at different temperatures using hydrazine hydrate as reducing agent. In this experiment, there are two oppositely moving 'diffusion-reaction' fronts and the temperature at which the both become comparable to each other, hollow structures are likely to be formed. Spectroscopically, the formation of hollow plasmonic nanostructures is indicated by the red-shift in the plasmon peak. The SPR peak is observed at 409 nm for the syntheses at 10 °C, 15 °C and 25 °C. But, the peak red-shifts to 423 nm at 20 °C. As the maximum redshift is observed at 20 °C, this is chosen as the synthesis temperature for rest of the experiments.

Elemental analysis by energy dispersive X-ray spectroscopy (EDX)

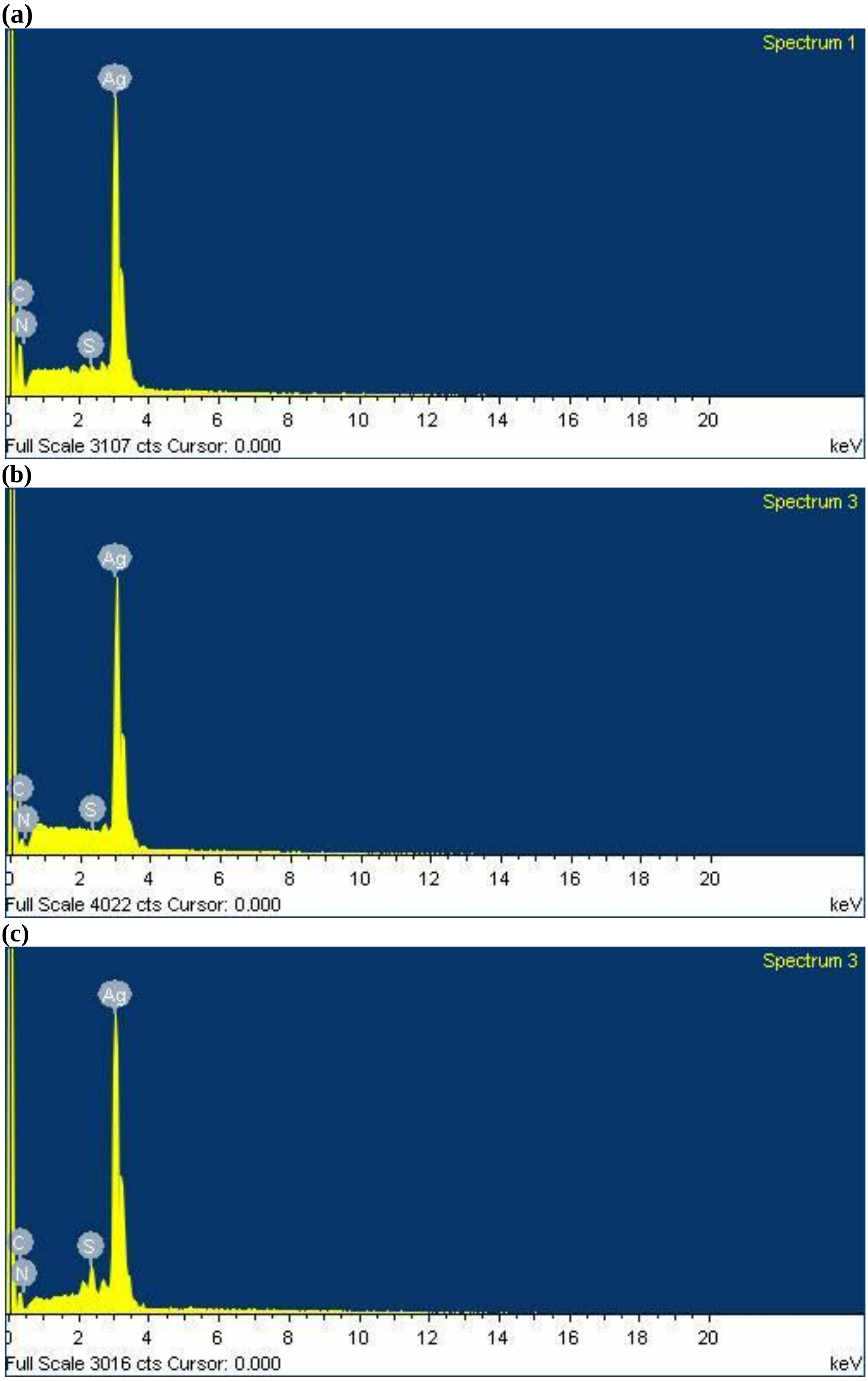

Figure S2. EDX spectra of hollow silver nanoshells having an aspect ratio of (a) 2.8, (b) 5 and (c) 4.2 . The TEM images of the samples is given in Figure 2, 4a and 4b, respectively of the main text. The samples were synthesized using citrate as stabilizer and hydrazine hydrate as reductant.

A dominant peak for Ag can be easily seen in all the samples. No peak for oxygen could be detected which means all the Ag_2O species have been reduced to metallic silver. After the synthesis, capping agent, citrate, was replaced with mercaptopyridine and extracted to organic solvent, toluene, for better stability of the nanoshells. Due to this reason, the peaks for sulphur and nitrogen are also observed in the EDX spectrum.

Effect of reductant concentration on plasmon peaks

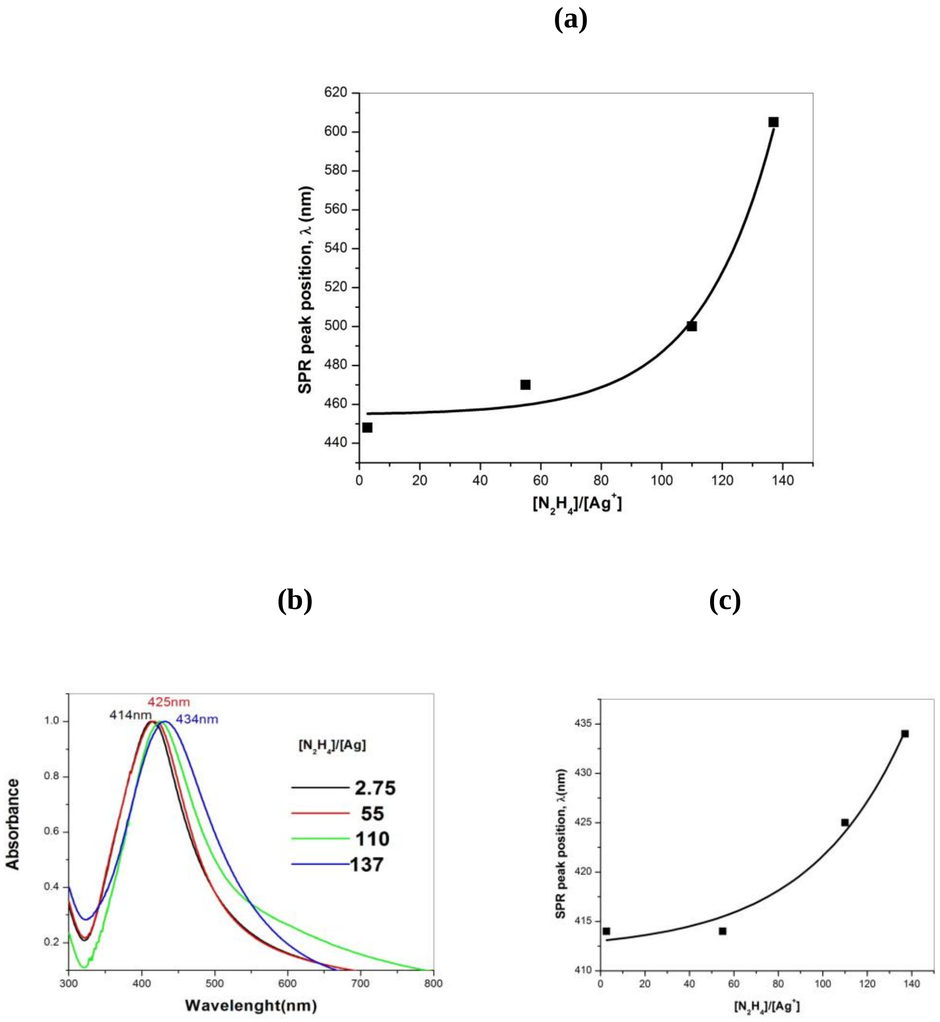

Figure S3. Variation of SPR peak with change in molar ratio of reductant/Ag+ ions, $[N_2H_4]/[Ag^+]$: (a) citrate used as stabilizer; (b), (c) thioglycolic acid (TGA) used as stabilizer.

The SPR peak was found to increase exponentially with change in the ratio of $[N_2H_4]/[Ag^+]$. When citrate was used as stabilizer, the SPR peak could be tuned in a wide range from 460 to 605 nm for a change in ratio from 2.75 to 137. In contrast, with thiglycollic acid as stabilizer, the SPR peak only moved from 414 to 434 nm for the same change in hydrazine concentration as shown in Figure S3. However, the variation of plamon peak with change in molar ratio exhibited an exponential profile as observed in case of citrate.

Characterization fo Ag_2O NPs:

Ag_2O NPs synthesized using citrate and hydrazine were characterized by TEM and dynamic light scattering techniques results of which are given in Figure S4. The average size determined from TEM images is 71±6 nm. The DLS measurements show the mean hydrodynamic diameter as 80 nm. From SAED pattern, the d-values were found to be 2.7, 2.3, 1.6 and 1.4 Å which correspond to the hkl planes of 111, 200, 220 and 311 respectively. This indicates that cubic Ag_2O NPs have cubic structure (space group $Pn\overline{3}$, JCPDS 76-1393).

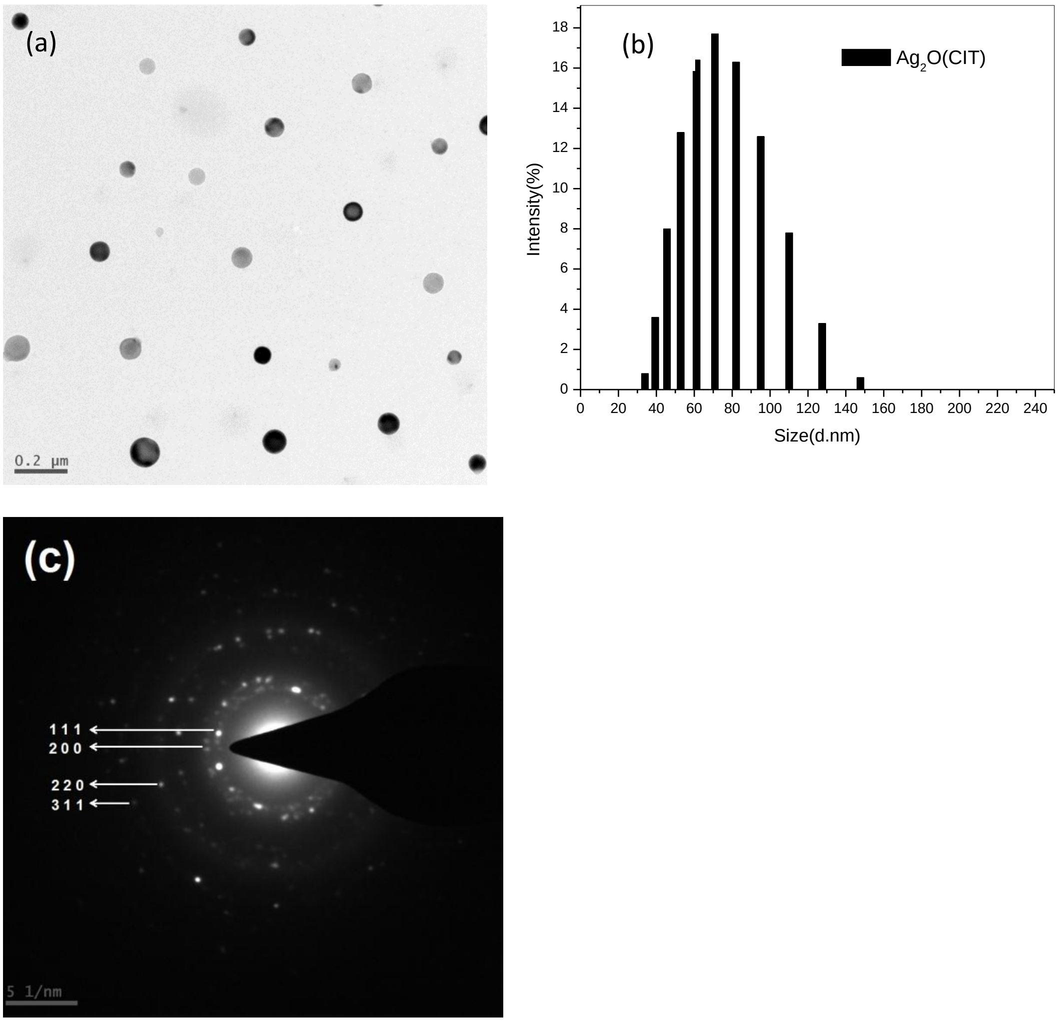

Figure S4. (a) TEM image of Ag_2O NPs prepared using citrate as stabilizer and hydrzine hydrate as reductant. (b) size distribution profile obtained by DLS technique. (c) Selected area electron diffraction (SAED) pattern for Ag_2O NPs.

Effect of weaker reducing agents on the nanoshell synthesis :

On carrying out reduction of Ag2O NPs using dextrose monohydrate in a fast-reverse addition mode, hollow nanoshells could not be obtained. Solid silver nanoparticles much smaller than Ag2O template NPs are formed as shown in the TEM images (Figure S5).

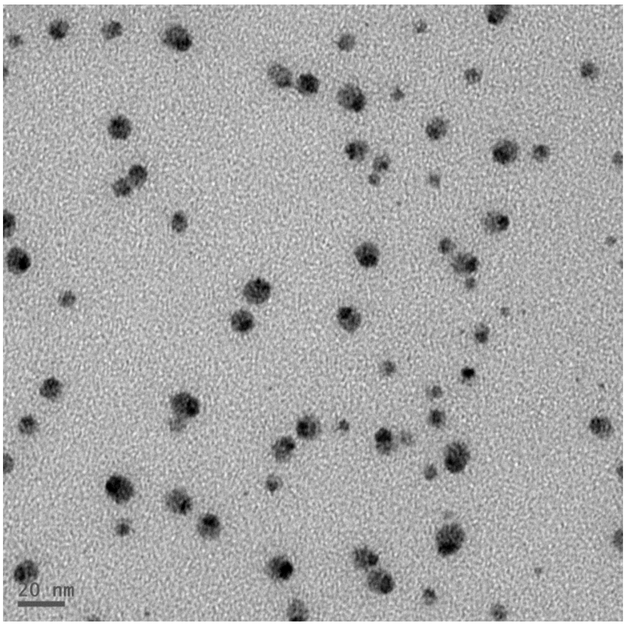

Figure S5. TEM image of Ag NPs formed due to reduction of Ag2O NPs by dextrose monohydrate in the fast-reverse addition mode.

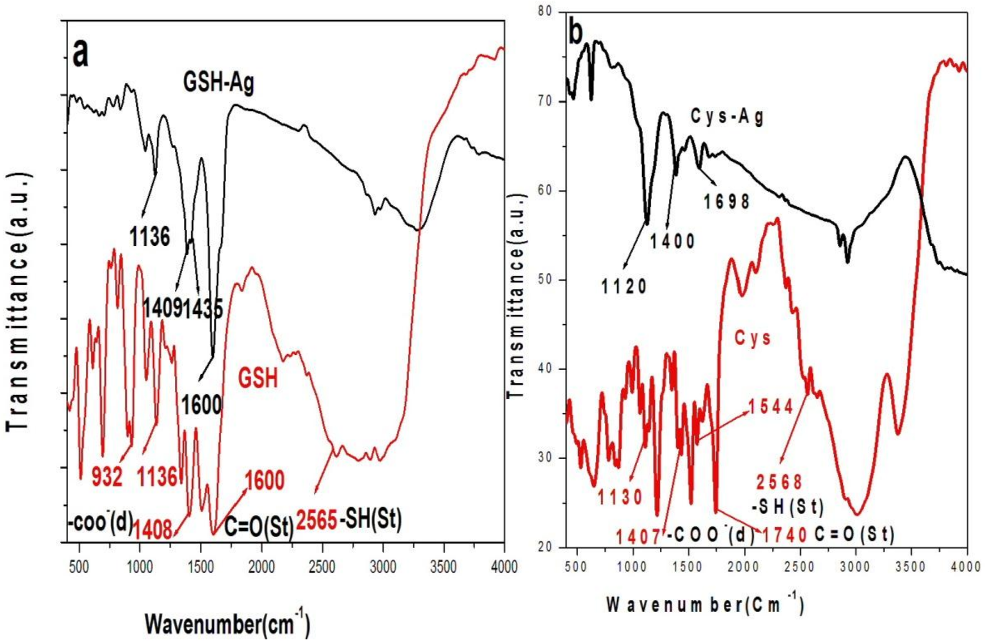

Figure S6. FTIR spectra of (a) Glutathione (GSH) and GSH-capped HAgNS, (b) Cysteine and cysteine capped HAgNS.

Comparison between nature of binding between Glutathione and some other thiols:

In case of GSH and cysteine, it is the thiol moiety that binds to the surface of nanoparticles. That's why the band at 2560 cm^{-1} and 932 cm^{-1} for –SH stretching and bending modes, respectively, disappear in the FTIR spectra of GSH -HAgNS or Cys-HAgNS. But, in comparison to other thiols, GSH-HAgNS shows some other notable changes. The broad band at 1408cm^{-1} in pure GSH that corresponds to –COO^{-} deformation splits into two peaks at 1409 cm^{-1} and 1435cm^{-1} in case of GSH-HAgNS. The observation suggests that the two terminal carboxylic group also interact with the nanoparticle surface. In contrast, the TGA-HAgNS which also has thiol and carboxyl group, does not show this peculiar feature associated with –COO^{-} deformation. It appears, the terminal carboxyl groups of thiols can interact with the particle surface only when the hydrocarbon chain is sufficiently long. In the case of GSH, the molecule is able to adopt a conformation that makes the binding of carboxylate groups to the particle surface feasible. For shorter chain thiols such as TGA, the required geometry puts up too much strain which makes the interaction of terminal carboxyl energetically unfavourable.

pH stability of hollow silver nanohells:

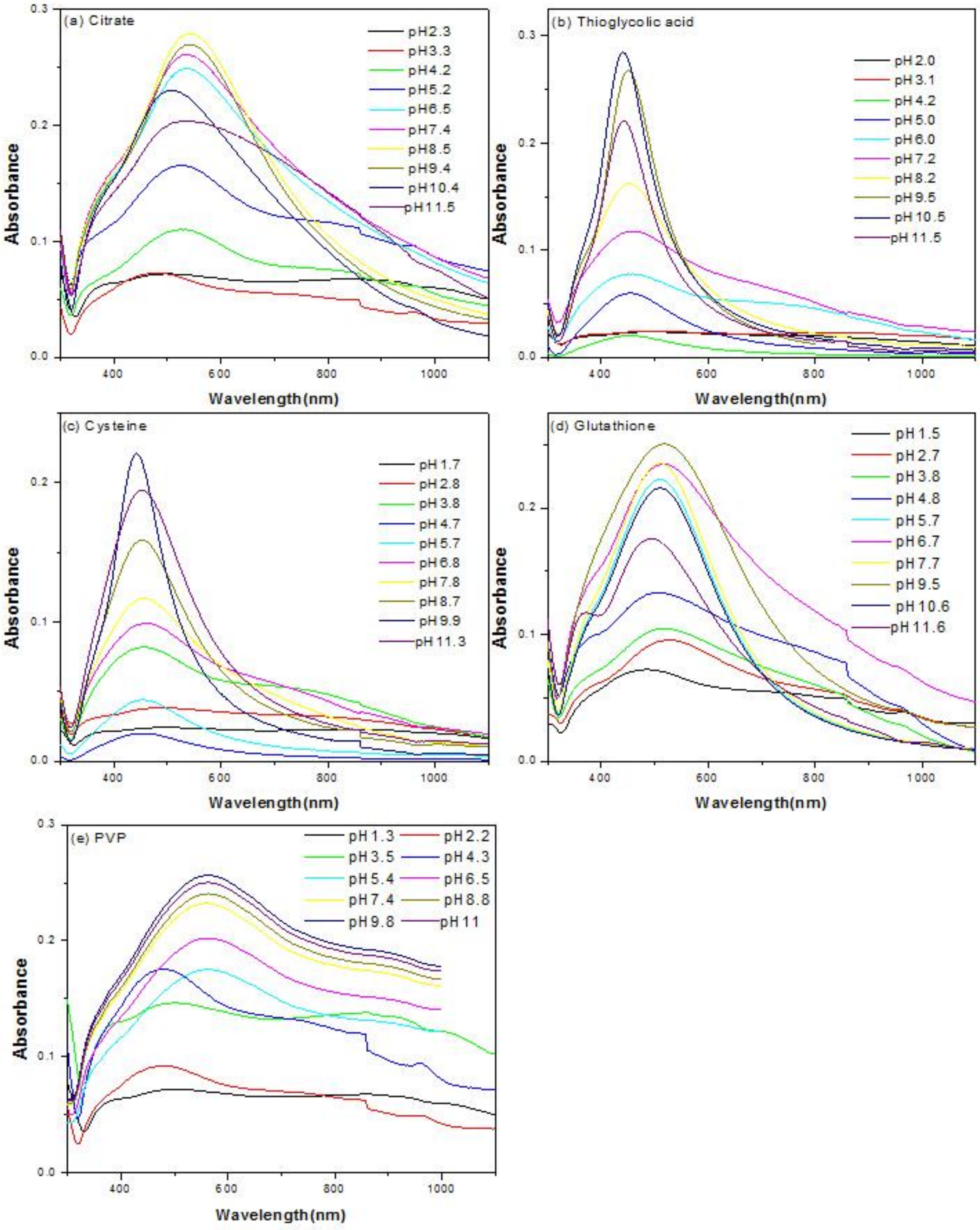

Figure S7. pH dependent UV-Vis absorption spectra of hollow nanoshells in presence of different stabilizing agents: (a) citrate, (b) thioglycolic acid, (c) cysteine, (d) glutathione and (e) polyvinylpyrrolidone (PVP)

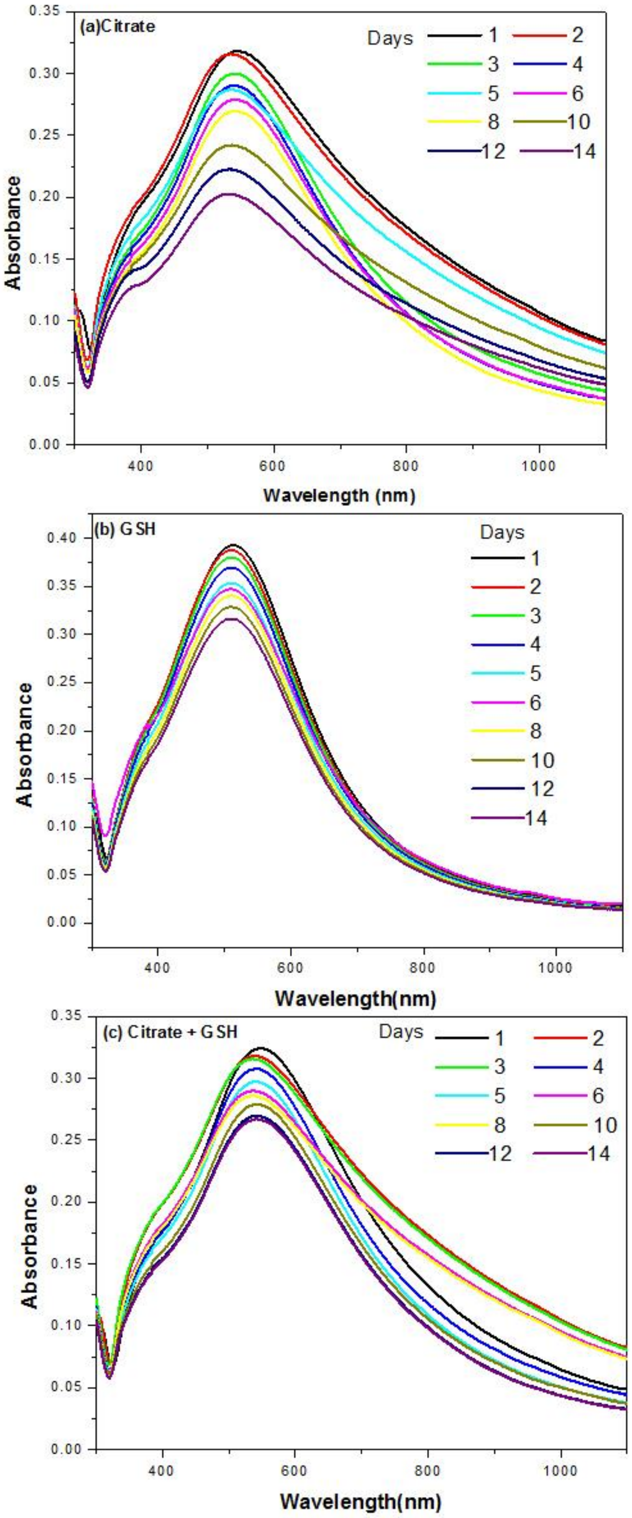

Figure S8. Variation in UV-Vis absorption spectra of hollow nanoshells at pH 7.4 during storage for two weeks in presence of different stabilizing agents: (a) citrate, (b) thioglycolic acid, (c) cysteine, (d) glutathione and (e) polyvinylpyrrolidone (PVP)

Table S1. SPR peak position for different sets of stabilizers and reducing agents in 'fast-normal' and 'fast-reverse' addition modes

Stabilizer	**Reducing agent**	**SPR Peak position (nm)**	
		Fast-Normal addition	**Fast-Reverse addition**
Citric Acid [a]	$N_2H_4.H_2O$	530	605
	Dextrose monohydrate	410	413
	L-ascorbic acid	400	400
	$NaBH_4$		550
Thioglycollic acid [b]	$N_2H_4.H_2O$	414	414
	$NaBH_4$	446	449
2-mercaptoethanol [b]	$N_2H_4.H_2O$	416	425
	$NaBH_4$	460	470
L-cysteine [b]	$N_2H_4.H_2O$	414nm	418nm
	$NaBH_4$	455nm	459nm
Glutathione (GSH) [b]	$N_2H_4.H_2O$	434nm	434nm
	$NaBH_4$	490nm	510nm
Glycine [a]	$N_2H_4.H_2O$	498nm	585nm
Tartaric acid [a]	$N_2H_4.H_2O$	500nm	595nm
Poly Vinyl Pyrolidone[a]	$N_2H_4.H_2O$	460nm	560nm

a: (50µL, 10 mM) **b**: (18µL, 10 mM)